



PERGAMON

Journal of Structural Geology 25 (2003) 903–908

**JOURNAL OF  
STRUCTURAL  
GEOLOGY**

[www.elsevier.com/locate/jsg](http://www.elsevier.com/locate/jsg)

# Direction of resolved shear stress: a construction and discussion

Norman Fry\*

*Laboratory for Strain Analysis, Department of Earth Sciences, Cardiff University, PO Box 914, Cardiff CF10 3YE, UK*

Received 7 August 2001; received in revised form 1 September 2002; accepted 11 September 2002

## Abstract

A simple construction facilitates identification of the direction of resolved shear stress for Andersonian conditions (in which one principal axis is vertical). A constructed horizontal ‘rake guide’, for specific stress and strike, will project perpendicularly onto any dipping plane as the direction of resolved shear stress. Consideration of rake guides, for different strikes for each fixed stress state, illustrates that tectonic regimes are identifiable by ranges, but not by individual values of rake. The ‘tectonic regime parameter’ and the ‘rake guide angle’ are useful parameters for Andersonian stress.

© 2002 Elsevier Science Ltd. All rights reserved.

*Keywords:* Shear stress; Tectonic regime; Stress regime; Fault slip

## 1. Introduction

### 1.1. Subject

The aim of this paper is to help clarify the relationship between the full three-dimensional stress state and the direction of resolved shear stress on a plane.

This relationship is easily misunderstood. For example, an observation that a fault displacement has normal sense might be thought to indicate a stress state in which the principal axis of maximum compression is near vertical. Such a deduction may be valid for newly created faults, in accord with Anderson’s (1905, 1951) theory. However, it cannot be relied upon when there is displacement on a pre-existing surface, such as reactivation of an earlier fault. For such cases, we follow Wallace (1951) and Bott (1959) in assuming that the fault motion is along the direction of maximum resolved shear stress. This may be down-dip with normal sense even if the compressive stress along a principal axis lying exactly vertical has a lower value than the average horizontal compression. Relationships that have already been demonstrated in the literature deserve greater currency.

This paper addresses stress states with a vertical principal direction, sometimes referred to as ‘Andersonian’ in recognition of the pioneering work of Anderson (1905),

necessitating consideration only of those orientations, directions and angles shown in Fig. 1.

### 1.2. Context

The geometry demonstrated here is implicit in generally accepted stress theory and has been illustrated in the comprehensive review of Andersonian stress by Célérier (1995). This paper introduces a new construction that is graphically and conceptually simple. It makes explicit the geometrical and physical significance of a relationship subsumed within the methods of Fry (1992) and Célérier (1995). It uses fuller illustration to extend discussion of ideas in Fry (1992), Célérier (1995) and Célérier and Séranne (2001).

### 1.3. Symbols, terms and conventions

Some conventions and most symbols follow Célérier (1995). Compression is positive, planar orientations are given by using strike, rather than the azimuth of the dip-direction, and the term ‘rake’ is used, rather than ‘pitch’.

However, the approach to signs of variables and to reference frames is different. The essence of this paper is the feasibility of construction using, as far as possible, only two dimensions. In so far as the two dimensions define a parametric space, positive coordinates are here taken as rightwards and upwards. In so far as they are real space, they represent the horizontal plane viewed from above, in which,

\* Tel.: +44-29-2087-5773, fax: +44-29-2087-4326.

E-mail address: FryN@cf.ac.uk (N. Fry).

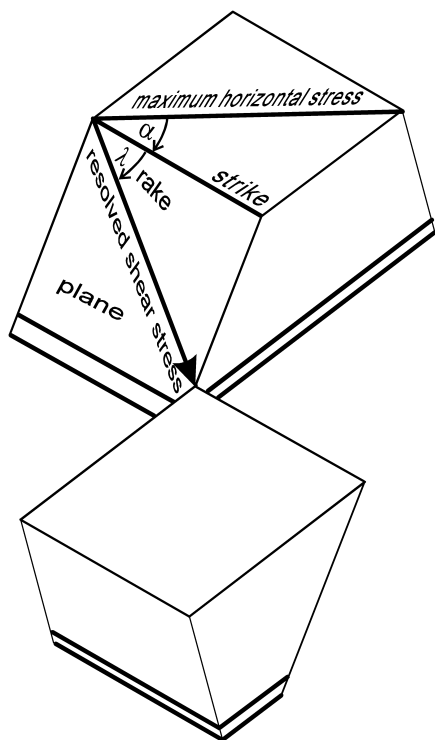


Fig. 1. Attitudes, directions and angles for Andersonian conditions. In the horizontal plane,  $\alpha$  is the angle (difference in bearing) from the greater of the two horizontal principal stresses to strike. The angle of rake,  $\lambda$ , is measured clockwise within the plane being considered, from strike with  $\lambda = 0$  for pure sinistral resolved shear stress.

by historical convention, angles (e.g. strike) are clockwise positive. This choice of the main symmetry plane of the Andersonian stress tensor renders consideration of reference frames in three dimensions (Célérier, 1995) unnecessary. The only essential excursions from horizontal are projections of angles in the horizontal to angles in dipping planes. Such projection conserves the sense of rotation, giving clockwise-positive angles of rake, for which it is convenient to take pure sinistral strike as the zero reference direction (Fig. 1). This usage is in agreement with convention for recording structural field data according to, for example, the Geological Society of London Handbooks by Barnes (1981) and McClay (1987). However, this convention is not universally acknowledged, and is contrary both to the clockwise from dextral, engineering, usage of, for example, Jaeger (1969) and to the anticlockwise, seismological, usage of, for example, Aki and Richards (1980) favoured by Célérier (1995). Readers are invited to modify the constructions in this paper to suit their own conventions.

The 'shape' or 'aspect ratio' of a stress tensor is often rendered as a ratio of differences of principal stresses called a 'stress ratio'. For Andersonian conditions, stress ratio functions that highlight the special status of the vertical axis have been variously defined and used by Armijo et al. (1982), Simón-Gómez (1986), Fry (1992) and others. The one used here is the 'tectonic regime parameter',  $\gamma$ , defined

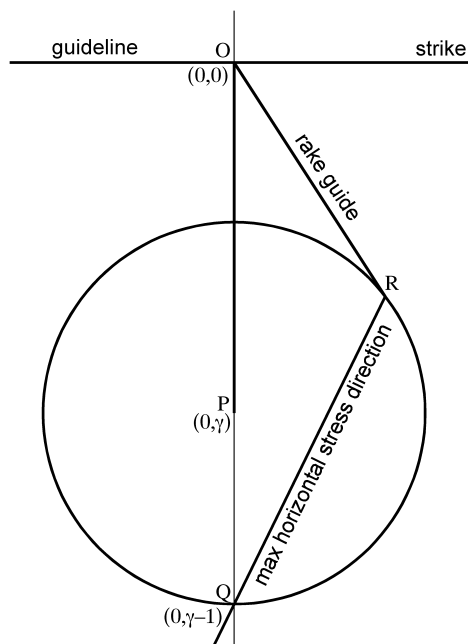


Fig. 2. Construction for direction of resolved shear stress on a plane. Line OP represents upward distance  $\gamma$ . The circle about P has unit radius at the same scale as OP. With the guideline along strike, dip towards the viewer and the maximum horizontal stress direction, QR, drawn in its true direction, OR is the direction of the 'rake guide', which will project normally onto the plane to give the direction of resolved shear stress.

by Célérier (1995) as:

$$\gamma = \frac{\sigma_{h1} + \sigma_{h2} - 2\sigma_v}{\sigma_{h1} - \sigma_{h2}}, \quad \gamma \in ] - \infty, +\infty[ \quad (1)$$

where subscript v indicates vertical, h horizontal and  $\sigma_{h1} \geq \sigma_{h2}$ .

## 2. Construction for resolved shear stress direction on a single plane

The following construction is illustrated in Fig. 2.

Draw a horizontal guideline on a piece of paper. From an origin, O, on this line, move a perpendicular distance, which at a suitable scale represents the value of  $\gamma$ . The point, P, so reached may lie either above or, as in Fig. 2, below the origin, according to whether  $\gamma$  is positive or negative, respectively. Draw a circle of unit radius centred on P, and mark the lowest point of the circle, Q.

Lie the paper horizontal and orient it with respect to the plane to be considered, so that the guideline is now along strike, with the plane dipping towards you. Draw a line from Q in the direction of the maximum horizontal stress, to intersect the circle at a second point, R. The line to R from the starting origin, O, gives the direction of what is here named the 'rake guide'. It is the horizontal direction that projects, normal to the dipping plane, to give the direction of resolved shear stress (OR projects to OS, in Fig. 3) in the

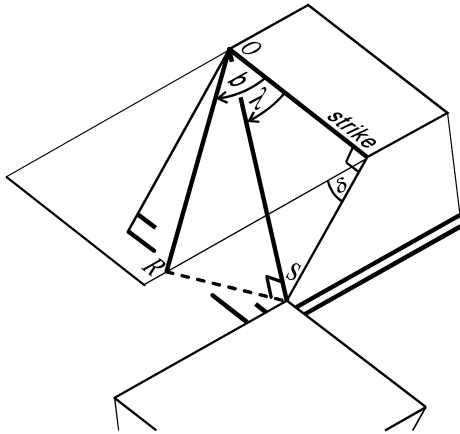


Fig. 3. The geometrical relationship between the rake guide, OR, as in Fig. 2, with a rake guide angle,  $b$ , and projection onto the plane to give the direction of resolved shear stress, OS, and its rake,  $\lambda$ . This geometry accords with  $\tan b = \tan \lambda / \cos \delta$ , where  $\delta$  is the angle of dip.

plane. It is also the true direction to which that of the resolved shear stress tends as dip of the plane tends to zero.

The mathematical relationships behind this construction are given later, in Section 5, as they apply equally to a modification to be presented in Section 3.

The rake guide constructed as above may lie in any direction, in any quadrant from the origin, dependent on the value of  $\gamma$  and the direction of the maximum stress in the horizontal plane. Projection to the direction of resolved shear stress, as in Fig. 3, does not change either the quadrant or, as pointed out by Célérier (1995), the horizontal component of rake, only the dip-direction component and, in consequence, the resultant direction within that quadrant.

### 3. Rake as a function of strike

#### 3.1. The modified geometrical construction

For the same tectonic regime parameter, it is possible to compile, onto one diagram of the type shown in Fig. 2, the directions of maximum horizontal stress and their corresponding rake guides for any number of planes. The resulting diagram would indeed show the variation of rake as a function of strike for a constant stress condition. However, it would do so by representing the variable, strike, by a constant direction and representing the constant, maximum horizontal stress direction, by a variable.

To provide rake as a function of strike in a more conventional manner, stress can be fixed by fixing the tectonic regime parameter (fixed position of the circle of Fig. 2) and fixing the direction of maximum horizontal compression, represented by a fixed reference line. This requires the construction of Fig. 2 to be modified by addition of a horizontal reference line through Q, and deletion of the label ‘max horizontal stress direction’, as in Fig. 4. The diagram is no longer oriented with respect to strike of a

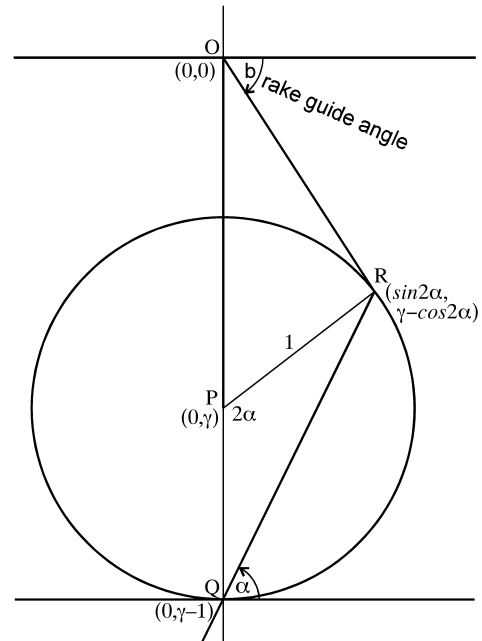


Fig. 4. Modified construction to enable rake guides to be constructed for more than one strike direction, for a common fixed  $\gamma$  and direction of maximum horizontal stress. Clockwise angle from direction of maximum horizontal stress to strike,  $\alpha$ , is plotted anticlockwise from the horizontal reference line through Q. For a particular  $\alpha$ , the resulting rake guide, OR, is at the correct rake guide angle,  $b$ , from the strike of the particular plane. Because the angle between PQ and PR is  $2\alpha$ , the coordinates of R are  $(\sin 2\alpha, \gamma - \cos 2\alpha)$ , such that the tangent of the rake guide angle,  $\tan b$ , has the correct value,  $-(\gamma - \cos 2\alpha) / \sin 2\alpha$ , for Eq. (3).

particular plane. Instead, the *clockwise* angle  $\alpha$  from the direction of maximum horizontal stress to strike of the plane (Fig. 1) is plotted *anticlockwise* from the horizontal reference line through Q to the line QR. Despite loss of real orientation with respect to any particular fault plane, the value of the angle  $b$  at point O, from the upper reference line to line OR in Fig. 4, remains correct, as the angle from strike to the rake guide. The result of this modified construction (Fig. 4) is the same geometry as in the lefthand columns of Figs. 12 and 13 of Célérier (1995).

#### 3.2. The rake guide angle

The clockwise angle from strike to a rake guide (Figs. 3 and 4) is named here the ‘rake guide angle’. This modified construction geometrically evaluates rake guide angle,  $b$ , as a function of  $\alpha$ , clockwise angle from maximum horizontal stress to strike. It is the geometric equivalent of the algebraic specifications given, with alternative symbolisms, by Fry (1992) and Célérier (1995). Figs. 3 and 4 demonstrate that the algebraic variable symbolised  $b$  by Fry (1992) and  $\lambda_0(\alpha, \gamma)$  by Célérier (1995), and its mapping to evaluate rake, have direct geometrical and physical meaning (Fig. 3) as the ‘rake guide angle’, and the process, resolving the rake guide’s in-plane component by normal projection, which gives the rake on the plane.

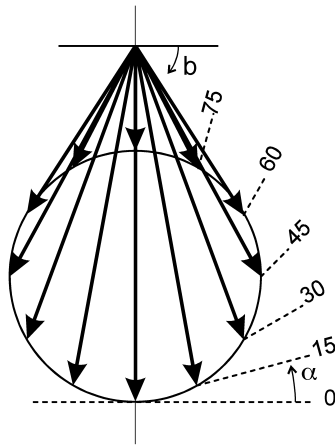


Fig. 5. Rake guides (arrows) constructed as in Fig. 4 for every  $15^\circ$  of  $\alpha$ , for one chosen value of tectonic regime parameter ( $\gamma = -11/6$ ).

### 3.3. Illustrating ranges of rake guide angles and rakes

If desired, lines joining the origin, O, to successive positions of R can be drawn to provide rake guides, at rake guide angles,  $b$ , for any number of strike values,  $\alpha$ . Fig. 5 shows rake guides for every  $15^\circ$  of  $\alpha$ , or alternatively, as viewed by C  lerier (1995), at every  $30^\circ$  of  $2\alpha$  measured at the centre of the circle. Projections of such a set of rake guides may be displayed for any particular angle of dip of a plane, or for a selection of dip angles, as in Figs. 12 and 13, respectively, of C  lerier (1995).

## 4. Concepts illustrated by the method

### 4.1. Regimes and rake ranges

Readers are advised to consult Harland and Bayly (1958), Armijo et al. (1982), Fry (1992) and C  lerier (1995) about historically used regimes and their names, and to refer to Table 2 in C  lerier (1995) for formal definitions of regime limits, which are not strictly adhered to in the simplified inequalities below. The three generally accepted stress regimes are characterised by different ranges of rake. Fig. 6 extends the scope of C  lerier's (1995) Fig. 13 to illustrate these differences more fully, as follows.

Stress states within the 'reverse' or 'compression' tectonic regime ( $\gamma > 1$ ; least compression vertical) give a reverse sense of dip-slip component on planes of all orientations. The higher the value of  $\gamma$ , the more restricted and close to up-dip the directions become.

Within the wrench regime ( $-1 < \gamma < 1$ ; vertical compression within the range of horizontal compressions) any stress state might produce an entire  $360^\circ$  range of angles of rake, although we should remember that the full range can only be realised as fault movement if frictional coefficient is very low.

Stress states within the 'normal' or 'extension' regime ( $\gamma < -1$ ; greatest compression vertical) give a normal

sense of dip-slip component on planes of all orientations. The more negative the value of  $\gamma$ , the more restricted and close to down-dip is the range of directions.

### 4.2. Variation, error and confidence in dip and stress ratio

Within the normal and reverse tectonic regimes ( $|\gamma| > 1$ ), increase in angle of dip of the plane increases the range of possible rake angles. A similar increase in range could be caused by a decrease in  $|\gamma|$ . This is illustrated in a very exaggerated form in Fig. 6 by, for example, the similarity of changing from ( $\gamma = 4, \delta = 0$ ) either to ( $\gamma = 2, \delta = 0$ ) or to ( $\gamma = 4, \delta = 60^\circ$ ). When analysing empirical data, effects of increase in dip and of decrease in  $|\gamma|$  cannot be entirely distinguished, because the assumption of verticality of a principal axis of stress may be only an approximation. Deviation of a principal axis from the vertical means that there is uncertainty in the value of the angle between the plane and the principal stresses, conceptually encapsulated as 'dip' in the discussion to this point. As a consequence, there will be uncertainty in the contribution of  $|\gamma|$  to the range of rake angles, and so in any estimation of  $\gamma$  from empirical data. C  lerier and S  ranne (2001) discuss departure from the assumed verticality of a principal stress axis and state that it can lead to a "poor estimate of the stress tensor aspect ratio". From the context of discussing a particular graphical procedure, their comment might appear to imply a weakness of their method. On the contrary, at least as far as normal and reverse tectonic regimes are concerned, their point is of general applicability to all estimations of  $\gamma$ , not particular to their method.

Within the wrench regime, uncertainty of the assumptions (effectively of 'dip') may affect the strike values at which the sense changes, between normal and reverse or between dextral and sinistral, and consequently lead to inaccuracy in estimation of the direction of maximum horizontal stress. However, it does not affect the possible  $360^\circ$  range of rakes except on planes of very low dip. Also, if deviation of an assumed principal axis is approximately towards or away from the direction of dip, illustrated grossly by change of row in Fig. 6, it does not affect the differences between the strike values at which there are changes of sense, from which  $\gamma$  may be estimated. Consequently, inaccuracy in the assumption of vertical stress may not detract from the estimation of  $\gamma$  for the wrench regime in the same way as for the normal and reverse regimes.

## 5. Mathematical considerations

C  lerier (1995) and C  lerier and S  ranne (2001) provide, in their Eq. (20) and Eq. (5), respectively, the down-dip component of the computed direction of resolved shear stress as  $(\cos 2\alpha - \gamma)\cos\delta$  and the rightward component (when dip is towards you) as  $\sin 2\alpha$ . The tangent of rake,  $\lambda$ ,

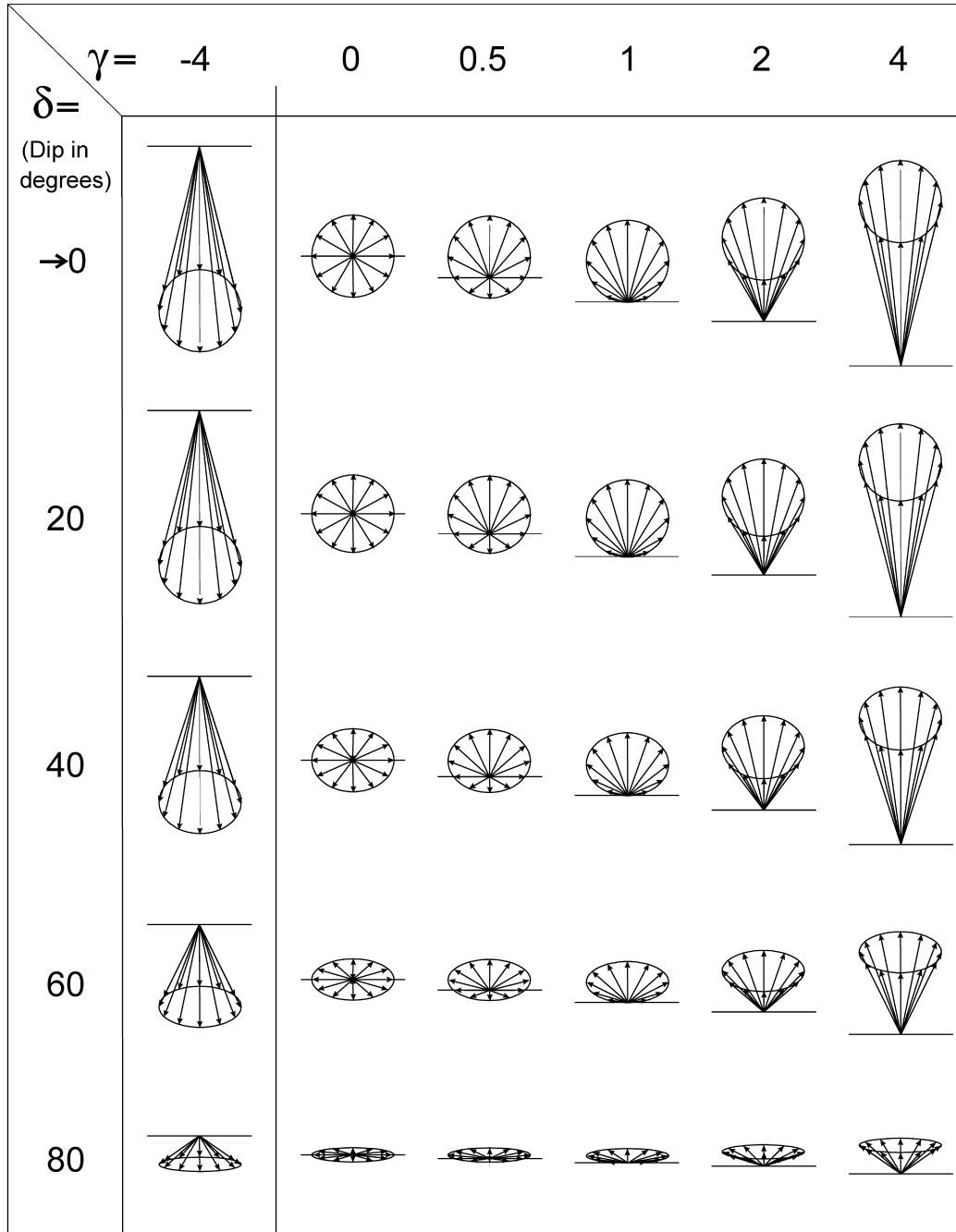


Fig. 6. Compilation of resolved shear stress directions and their rake angles for every 15° of  $\alpha$ , for selected values of tectonic regime parameter,  $\gamma$ , and dip,  $\delta$ . For each  $(\gamma, \delta)$  the horizontal reference line represents strike on a plane dipping towards the viewer. Each arrow is the direction, correct relative to its strike, of the resolved shear stress for  $\alpha$  at one of the 15° steps as in Fig. 5. Only one negative value of  $\gamma$  is shown ( $\gamma = -4$ ), to illustrate that the pattern of directions is the same as for positive  $\gamma$  of the same absolute value, mirrored through the horizontal. However, for negative  $\gamma$ , angles  $\alpha$  still start with  $\alpha = 0$  at the lowest point of the circle/ellipse and increase anticlockwise. Note that for  $|\gamma| < 1$ , corresponding to the entire range of the wrench regime, all 360° of rake are theoretically possible for all dips and particular  $\gamma$  values within the range, whereas for  $|\gamma| > 1$  the range of rakes is limited to 180° or less, of either normal or reverse sense in accord with the regime, and becomes increasingly constrained as  $|\gamma|$  increases and as  $\delta$  decreases.

is the ratio of these two components. Thus

$$\frac{\tan \lambda}{\cos \delta} = \frac{-(\gamma - \cos 2\alpha)}{\sin 2\alpha} \quad (2)$$

Eq. (2) may alternatively be derived from the equation into which Fry (1992) introduced angle  $b$ , with necessary

substitution of symbols:  $-\alpha$  for  $\lambda$ ,  $\lambda$  for  $\omega$ ,  $\delta$  for  $d$  and  $\gamma$  for  $(-\sqrt{3}\tan F)$ .

As already discussed in Section 3.2, the left-hand side of Eq. (2) has direct physical meaning. Equating it to  $\tan b$  (Fry, 1992), leads to the relationship illustrated in Fig. 3, where  $b$  is the rake guide angle. Ability to

separate out the term in  $\delta$  from Eq. (2) also means that, in reviewing how each parameter affects rake, it is convenient to evaluate and illustrate the right-hand side first, corresponding to the top row of Fig. 6, and then, for all illustrated combinations of tectonic regime parameter  $\gamma$  and strike  $\alpha$ , to consider variation with dip  $\delta$ , as lower in Fig. 6.

Rake  $\lambda$  is defined here as positive clockwise from pure sinistral (Fig. 1). For the sign of the rake guide angle,  $b$ , also positive clockwise, to conform to that for rake  $\lambda$ , its tangent is the ratio of the downward to the rightward component of resolved shear stress (Figs. 3 and 4). As positive  $\gamma$  has been plotted upwards, the downward component of rake is represented by the negative of this coordinate for point R in Fig. 4. Also, note that the coordinates of points O, P, Q, R in Fig. 4 apply unchanged in Fig. 2, as the difference between these plots—the reversal of the rotation sense of angle  $\alpha$ —does not affect the trigonometrical functions giving their coordinates. Both constructions (Figs. 2 and 4) achieve coordinates of R such that:

$$\tan b = \frac{-(\gamma - \cos 2\alpha)}{\sin 2\alpha} \quad (3)$$

as required by the relationship in Eq. (2) and Fig. 3. While it was initially inconvenient to introduce a negative value of  $\gamma$  in Fig. 2, this provided the positive values for both top and bottom of the right-hand side of Eqs. (2) and (3), according with the positive rake illustrated.

Whereas the constructions proposed in this paper provide for the full 360° possible range of angles, Eqs. (2) and (3) only provide  $b$  and  $\lambda$  within a range of 180°. Full algebraic treatment of conditions for addition of 180° has been given by Célérier (1995).

## 6. Conclusions

1. For stress conditions with one vertical principal axis, known as Andersonian, Célérier's (1995) 'tectonic regime parameter',  $\gamma$ , is an advantageous means of summarising the shape of the stress tensor.
2. Graphical construction of one or more 'rake guides', as in Figs. 2, 4 and 5 and in Figs. 12 and 13 of Célérier (1995), provides a basis for appreciation of the relationship between stress tensor and the rake of resolved shear stress on a plane. Unlike previously published constructions for direction of shear, construction of rake guides does not require prior trigonometrical calculation. Any trigonometry is relegated to the later, conceptually simple step of projection from horizontal to a dipping plane.
3. The 'rake guide angle' ( $b$  of Fry (1992) and Fig. 4;  $\lambda_0(\alpha, \gamma)$  of Célérier (1995)) and its mapping to give rake, have direct geometrical and physical meanings (Fig. 3). Rake guide angle is a useful intermediate parameter for

consideration of the relationship between stress tensor and the rake of resolved shear stress on a plane. This usefulness arises because projection, encapsulated algebraically by the term  $\cos \delta$ , is separable from the contributions of stress state and orientation, specified algebraically by terms in  $\gamma$  and  $\alpha$ .

4. The method introduced by Célérier (1995) and illustrated in Fig. 6 is a useful demonstration of how the ranges of rake angles vary with tectonic regime parameter,  $\gamma$ , strike,  $\alpha$  and dip,  $\delta$ .
5. As illustrated in Fig. 6, the three historically accepted tectonic regimes for Andersonian conditions are characterised by qualitatively distinct types of range of possible rake angles.

## Acknowledgements

Bernard Célérier's thorough review was extremely valuable, particularly in prompting clarifications and improvements in the justification of the conceptual basis of this paper.

## References

- Aki, K., Richards, P.G., 1980. Quantitative Seismology: Theory and Methods, W.H. Freeman and Company, San Francisco.
- Anderson, E.M., 1905. The dynamics of faulting. Transactions of the Edinburgh Geological Society 8, 387–402.
- Anderson, E.M., 1951. The Dynamics of Faulting and Dyke Formation with Applications to Britain, 2nd Ed, Oliver and Boyd, Edinburgh.
- Armijo, R., Carey, E., Cisternas, A., 1982. The inverse problem in microtectonics and the separation of tectonic phases. Tectonophysics 82, 145–160.
- Barnes, J.W., 1981. Basic Geological Mapping, Geological Society of London Handbook Series, Open University Press, Milton Keynes and Wiley, New York.
- Bott, M.H.P., 1959. The mechanics of oblique slip faulting. Geological Magazine 96, 109–117.
- Célérier, B., 1995. Tectonic regime and slip orientation of reactivated faults. Geophysical Journal International 121, 143–161.
- Célérier, B., Séranne, M., 2001. Breddin's graph for tectonic regimes. Journal of Structural Geology 23, 789–801.
- Fry, N., 1992. Stress ratio determinations from striated faults: a spherical plot for cases of near-vertical principal stress. Journal of Structural Geology 14, 1121–1131.
- Harland, W.B., Bayly, M.B., 1958. Tectonic regimes. Geological Magazine 95, 89–104.
- Jaeger, J.C., 1969. Elasticity, Fracture and Flow with Engineering and Geological Applications, Chapman and Hall, London.
- McClay, K.R., 1987. The Mapping of Geological Structures, Geological Society of London Handbook Series, Open University Press, Milton Keynes and Wiley, New York.
- Simón-Gómez, J.L., 1986. Analysis of a gradual change in stress regime (example from the Eastern Iberian chain, Spain). Tectonophysics 124, 37–53.
- Wallace, R.E., 1951. Geometry of shearing stress and relation to faulting. Journal of Geology 59, 118–130.